Clays and Clay Minerals, Vol. 53, No. 6, 572–579, 2005.

THE EFFECT OF MICROBIAL FE(III) REDUCTION ON SMECTITE FLOCCULATION

JIN-WOOK KIM[1,*], YOKO FURUKAWA[1], HAILIANG DONG[2] AND STEVEN W. NEWELL[1]

[1] Naval Research Laboratory, Seafloor Sciences Branch, Stennis Space Center, MS 39529, USA
[2] Department of Geology, Miami University, Oxford, OH 45056, USA

Abstract—This study was undertaken to investigate the changes in flocculation properties of Fe-rich smectite (nontronite, NAu-1) suspensions, including settling velocity, aggregate size and floc architecture associated with microbial Fe(III)-reduction in the smectite structure. The dissimilatory Fe-reducing bacterium *Shewanella oneidensis* MR-1 was incubated with lactate as the electron donor and structural Fe(III) as the sole electron acceptor for 3, 12, 24 and 48 h in an anaerobic chamber. Two controls were prepared; the first was identical to the experimental treatments except that heat-killed cells were used (non-reduced control), and the second control was the same as the first except that the incubation was carried out in an aerobic environment. The extent of Fe(III) reduction for the 48 h incubation was observed to reach up to 18%. Neither the non-reduced control nor the aerobically inoculated sample showed Fe(III) reduction. Compared with the non-reduced control, there was a 2.7 μm increase in mean aggregate size and a 30-fold increase in average settling velocity in the bioreduced smectite suspensions as measured using a Micromeritics Sedigraph®. The aerobically inoculated smectite showed a similar aggregate-size distribution to that of the non-reduced control. Significant changes in physical properties of smectite suspensions induced by microbial Fe(III) reduction were measured directly using transmission electron microscopy. The floc architecture of bioreduced smectite revealed less open structures compared to those of a non-reduced control. The aspect ratio (thickness/length) of individual smectite particle increased from 0.11 for the non-reduced control to 0.18 on average for the bioreduced smectite suspensions. The effects of pH on the clay flocculation were minimal in this study because the value of pH remained nearly constant at pH = 7.0–7.3 before and after the experiments. We therefore suggest that the increase in net negative charge caused by microbial Fe(III) reduction significantly promoted clay flocculation by increasing the electrochemical attraction in the smectite suspensions.

Key Words—Fe(III) Reduction, Flocculation, Micromeritics Sedigraph®, Nontronite (NAu-1), *Shewanella oneidensis* MR-1, Smectite, Transmission Electron Microscopy (TEM).

INTRODUCTION

The repackaging of suspended particles into large aggregate particles called flocs (Kranck and Milligan, 1992), affects the transport rate (McCave, 1975) and incorporation of biogenic and lithogenic particles. Association of particles and reactive chemical species into large flocs speeds up the vertical transfer of these materials (Hill, 1996). The flocculation process is often employed in gravitational settling for wastewater treatment in industries (Droppo *et al*., 2002). Flocculation is also responsible for the variability of shallow marine sediment structure and stability including shear strength and compressibility (Theilen and Pecher, 1991). Thus, understanding the flocculation processes, *e.g.* the prediction of the transport and fate of river-borne fine-grained sediments, has been a major interest of ocean scientists and engineers. Recent studies focused on the dynamics (transport/settling) of marine particle flocs in various sedimentary environments (Traykovski *et al*., 2000; Orton and Kineke, 2001; Allison *et al*., 2000; Hill *et al*., 2001), and many theoretical and laboratory studies showed the physical chemistry and fluid dynamics of interaction among sedimentary particles (Manning and Dyer, 1999; Brassard and Fish, 2000; Tombacz *et al*., 2001). However, previous studies paid little attention to some of the key variables important in the actual sedimentary environments such as a variability of particle compositions (*e.g.* bacteria, particulate organic matter and clay mineralogy) and temporal and spatial dynamics of redox chemistry controlled by the microbial diagenesis.

Particles coated with organic molecules from terrestrial plant degradation and bacterial exopolymer exudates may affect the efficiency of aggregation (Eisma *et al*., 1983). Bacteria are ubiquitous in soil and sediments, and have been shown to reduce octahedral Fe(III) effectively in clays causing surface-charge increase (Stucki *et al*., 1987; Wu *et al*., 1988; Gates *et al*., 1993; Kostka *et al*., 1996). Kim *et al*. (2003, 2004) reported that the smectite structure was altered through reductive dissolution by addition of the Fe-reducing bacterium (FeRB) *Shewanella oneidensis* MR-1. In addition, the surface chemistry of clay particles is altered when Fe(III) in the clay structure is respired by bacteria in an oxygen-depleted environment (Kostka *et al*., 1999). However, few studies have demonstrated the role of microbial Fe(III) reduction in clay flocculation

* E-mail address of corresponding author:
jkim@nrlssc.navy.mil
DOI: 10.1346/CCMN.2005.0530603

Copyright © 2005, The Clay Minerals Society

https://doi.org/10.1346/CCMN.2005.0530603 Published online by Cambridge University Press

properties, including settling velocity, floc architecture or the flocculation mechanisms. Furthermore, few direct observations of suspended particles were made.

In this study, the microbiological factor, especially microbial Fe(III) reduction in controlling particle flocculation, was investigated through direct transmission electron microscopy (TEM) observations on the physical properties of clay suspensions as well as floc architectures. The changes in the physical properties of clay suspensions induced by microbial Fe(III) reduction, including clay-packet size and structure, were measured on the TEM lattice-fringe images. In addition, changes in the aggregate-size distributions and settling velocity of particles were measured for variable durations of microbial Fe(III) reduction using a Micromeritics Sedigraph®. This study, therefore, attempted to quantify the flocculation behaviors of clay particles in microbially induced redox regimes in a bench-top environment.

MATERIAL AND METHODS

Clay mineral preparation

Nontronite from Uley graphite mine, South Australia (The Clay Minerals Society Reference Clay, NAu-1) (Keeling *et al.*, 2000) was used in this study. The <2 μm clay fraction (in suspension) was separated using the pipette method, and then air dried after centrifugation. Note that chemical treatment or oven-dry processing was not carried out during grain-size fractionation to minimize the alteration (if any) of its natural state. Powdered specimens (grain size <2 μm) were then sterilized by a 5 min exposure to microwave radiation (Keller *et al.*, 1988), and sterility was confirmed by lack of bacterial growth in LB broth following a 48 h incubation at 22ºC in the dark under aerobic conditions (95% N_2/5% H_2). Three aliquots each of 2.58 g of sterilized clay were prepared using a chemical balance.

Reduction experiment

The Fe(III)-reducing bacterium *S. oneidensis* strain MR-1, previously isolated from anoxic sediment (Myers and Nealson, 1988), was maintained aerobically on Luria-Bertani (LB) agar at 22ºC in the dark. The conditions for clay-reduction experiments were modified (Kostka *et al.*, 1999) and are described elsewhere (Kim *et al.*, 2003, 2004). The same amount of sterilized nontronite (2.58 g) and initial cell density of 2×10^8 cells/mL were used in three sets of experiments, including: (1) bioreduced smectite (BS), with variable incubation time (3, 12, 24 and 48 h) under anaerobic conditions: bacteria and smectite (as the sole electron acceptor) were added to 50 mL of fresh M1 media containing 20 mM lactate; (2) non-reduced control (NC), containing microwave radiation heat-killed bacterial cells, M1 medium plus lactate (20 mM) and smectite prepared the same way as for the anaerobic condition; and (3) aerobically inoculated smectite (AIS), the mixture of smectite and *S. oneidensis* in M1 media plus lactate (20 mM) was exposed to aerobic conditions for 48 h during which *S. oneidensis* respired oxygen rather than the Fe(III) in the smectite structure. The pH of the initial aqueous phase was 7.3. No attempt was made to buffer the pH value during the batch incubations and the pH value after the 48 h incubation was determined to be 7.0 by a pH probe.

Ferrozine assay

The extent of microbial Fe(III) reduction of smectite was monitored by measuring Fe(II) production. At select time points, 0.1 mL of cell-mineral suspension, sampled with a sterile syringe, was added to a plastic tube containing 0.1 mL of 1 N Ultrex HCl. The cell-mineral suspension was allowed to stand in HCl for 24 h before analyzing for Fe(II) concentration (Dong *et al.*, 2003). This extraction is termed the 0.5 N HCl extraction. The concentration of aqueous Fe(II) was determined by removing the solids through centrifugation in an anaerobic glove box followed by acidification and direct current plasma emission spectrometry.

Settling experiments

The aggregate-size distribution of each set of samples (BS, NC and AIS) was measured using a Micromeritics Sedigraph Model 5000® (Micromeritics, Norcross, Georgia). Samples were transferred from an anaerobic chamber to the sedigraph using the GasPak 100 System (BBL, Becton Dickinson Microbiology Systems, Cockeysville, Maryland) to preserve the redox state. The settling velocity at 50 cumulative mass percentage was determined based on 10 cm depth of sample, a temperature of 23º, 2.65 g/cc average grain density and Stokes' Law.

Transmission electron microscopy

Nanoplast-embedded and microtome-sliced smectite samples were prepared for TEM analyses. A total of 258 clay packets in BS and NC samples were measured on photographic negatives of lattice-fringe images using a microfiche reader. Most measurements were accomplished by measuring the thickness perpendicular to c^* and the length parallel to c^* across grain boundaries defined by small angles, concentrations of edge dislocations, tapering fringes in sequences of layers, or strong image contrast between lattice fringes as described by Kim *et al.* (1995) and Kim and Peacor (2002). The aspect ratio (thickness/length) of smectite grains in BS and NC samples was measured on the TEM lattice-fringe images. The evolution of floc architecture associated with microbial activity was also observed. A JEOL 3010 TEM operating at 300 keV with a LaB_6 filament was used for all TEM analyses in this study.

Microelectrophoresis

In order to measure the surface charge of the bioreduced smectite samples directly, electrophoretic mobility measurements were carried out for the samples

https://doi.org/10.1346/CCMN.2005.0530603 Published online by Cambridge University Press

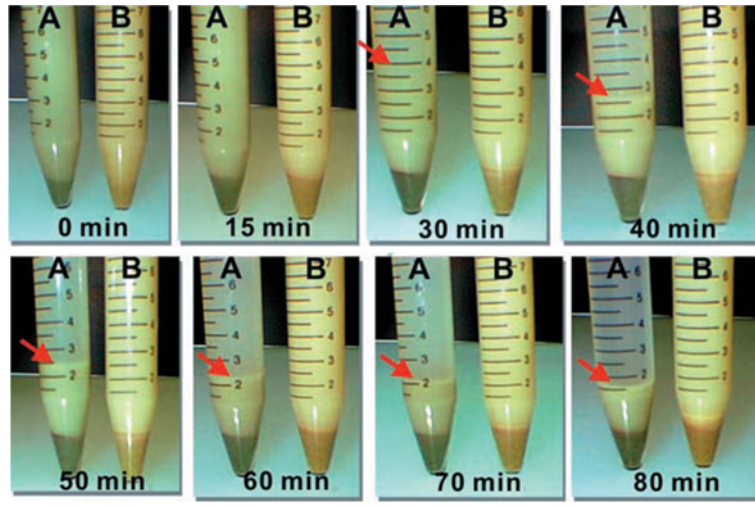


Figure 1. Bench-top experiment of settling behavior of bioreduced smectite (BS) in Tube A and non-reduced control (NC) suspensions in Tube B. Following 48 h incubation of *S. oneidensis* with nontronite (NAu-1), a substantial color change of BS occurred in Tube A as compared to NC in Tube B, suggesting microbial reduction of structural Fe(III) in the clay. Clay suspensions in Tubes A and B were observed for 80 min after being shaken homogeneously. The BS suspensions are flocculated and settled faster while the NC suspensions remained dispersed in the water column (see arrows showing the boundary of suspension).

in M1 medium with a Coulter DELSA 440 SX (Coulter Corporation, Miami, FL). Some samples (24 and 48 h) showed rapid settling. In that case, both suspensions and settled particles at the bottom were measured to evaluate the sample in homogeneity. The experimental conditions were as follows: temperature: 25ºC, frequency range: 500 Hz, electric field strength: 6 V, on-time: 2.5 s, and off-time 0.5 s. Typical temperature drifts within a single experiment were <0.1ºC so the effects of convection arising from Joule heating were minimized. Mobility measurements of standard carboxylate-modified polystyrene latex particles (nominal diameter = 300 nm) in 0.01 M sodium phosphate buffer at pH 7 were made periodically to check the stability of the DELSA instrument. The principles and other conditions have been described elsewhere (Dong, 2002).

RESULTS

Flocculation

Following 48 h of incubation of *S. oneidensis* with nontronite (Nau-1), a substantial color change of BS occurred in Tube A compared to NC in Tube B in Figure 1, suggesting the microbial reduction of structural Fe(III) in the clay. Indeed, the extent of Fe(III) reduction in BS was measured to reach 18% while no Fe(III) reduction occurred in NC or in aerobically inoculated smectite (AIS) as shown in Figure 2. In order to demonstrate the evolution in clay flocculation associated with microbial Fe(III) reduction, clay suspensions in Tube A and Tube B were observed for 80 min after being shaken homogeneously as shown in Figure 1. In Tube A, BS suspensions began to flocculate and settle in 30 min as indicated by the arrow, and then most suspensions were flocculated and settled in 80 min (note that the supernatant water appears clear). In contrast, NC suspensions remained dispersed in the water column in Tube B. This settling experiment yields a major hypothesis to be tested: the aggregation properties of sedimentary particles are strongly influenced by the microbial respiration of Fe, which is a ubiquitous process in cohesive sediments in anaerobic environments.

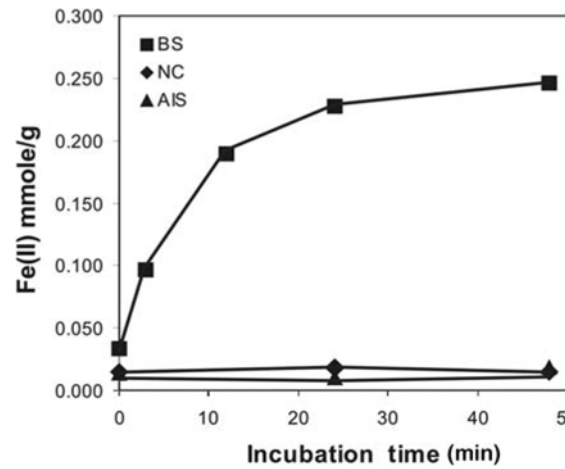


Figure 2. Change of HCl-extractable Fe(II) with time in the non-reduced control (NC), bioreduced smectite (BS), and aerobically inoculated smectite (AIS). The measured HCl-extractable Fe(II) concentration (mM) was normalized to milligrams of smectite in each tube, and reported as mmol/g. The extent of reduction by the end of incubation reached 18%, based on the measured Fe(III) concentration and the amount of smectite used in the tubes. The vertical errors are typically <10%.

https://doi.org/10.1346/CCMN.2005.0530603 Published online by Cambridge University Press

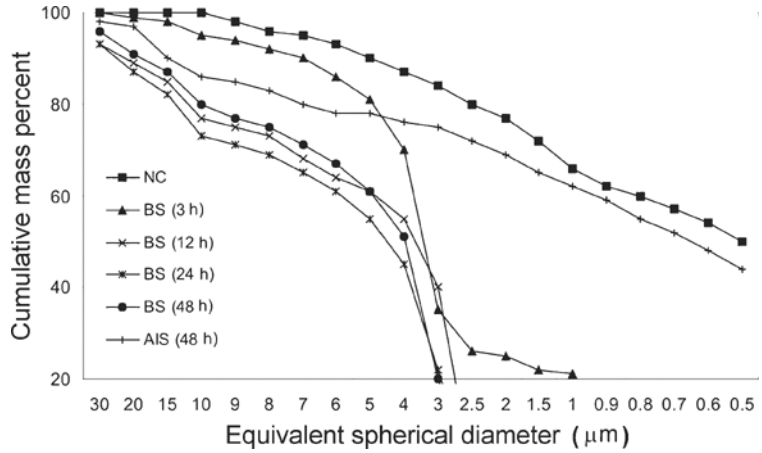


Figure 3. Aggregate size distribution of non-reduced control (NC), bioreduced smectite (BS) suspension (variable incubation time from 3 to 48 h) and aerobically inoculated smectite (AIS) suspensions using a Micromeritics Sedigaph. The average aggregate size was measured at 50% cumulative mass % and settling velocity was calculated using Stokes' law.

Aggregate-size distributions (ASDs)

The aggregate-size distributions of BS for the various incubation times (3–48 h) were displayed in comparison to those of NC and AIS in Figure 3. The ASDs of BS suspensions (12, 24 and 48 h incubation) show a similar pattern, probably due to the similar Fe-reduction state, but they are clearly differentiated from that of NC. The ASD of BS for a short-term incubation (3 h incubation) is more like an intermediate pattern between NC and BS (12, 24 and 48 h incubation). The BS suspensions show the aggregate size ranging from 2.5 to 4 μm in equivalent spherical diameter at 50 cumulative mass percent, which is 5–8 times larger than the NC suspensions (0.5 μm). The calculated mean settling velocity of BS is 6.9×10^{-4} cm/s based on a temperature of 25°C, average grain density = 2.65 g/cc, and the average grain size = 3.2 μm, while a 2.1×10^{-5} cm/s settling velocity is calculated for NC with average grain-size of 0.5 μm. Furthermore, AIS (average grain size = 0.6 μm and settling velocity = 2.6×10^{-5} cm/s) yielded an ASD pattern corresponding to smaller aggregates than those yielded by BS and similar to that of NC as shown in Figure 3.

TEM analyses

The packet-size distributions and the aspect ratio of smectite grains in BS and NC were plotted in Figures 4a and 4b, respectively. A total of 120 (NC) and 138 (BS) smectite grains were measured on the TEM lattice-fringe images. The example of the direct TEM measurements of smectite packet thickness (perpendicular to c^*) and length (parallel to c^*) is demonstrated in Figure 5. The inset figures are the enlarged images of the outlined areas, showing the lattice fringes and the packet boundaries. The longer arrows indicate the lengths of smectite packets. As shown in Figure 4a, mean packet thickness of smectite increased from 11.4 nm to 23.9 nm following microbial Fe(III) reduction. The increase in aspect ratios of smectite

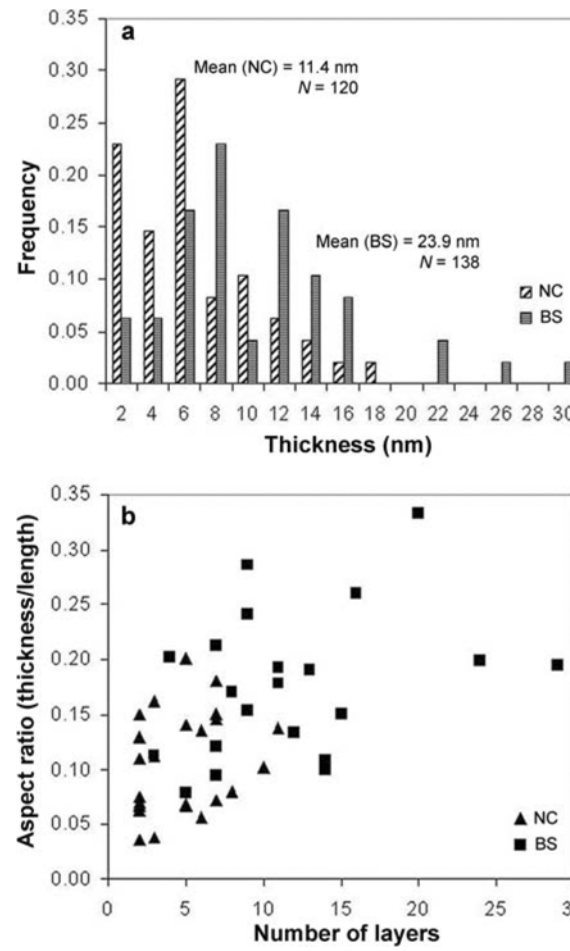


Figure 4. (a) The packet-size distribution and (b) aspect ratio of bioreduced smectite (BS) and non-reduced control (NC) showing an increase in mean packet size (11.4 nm to 23.9 nm) and aspect ratio (0.11 to 0.18). The errors of the measurements are typically ±5%. The measurements were made on TEM lattice-fringe images using a microfiche reader.

https://doi.org/10.1346/CCMN.2005.0530603 Published online by Cambridge University Press

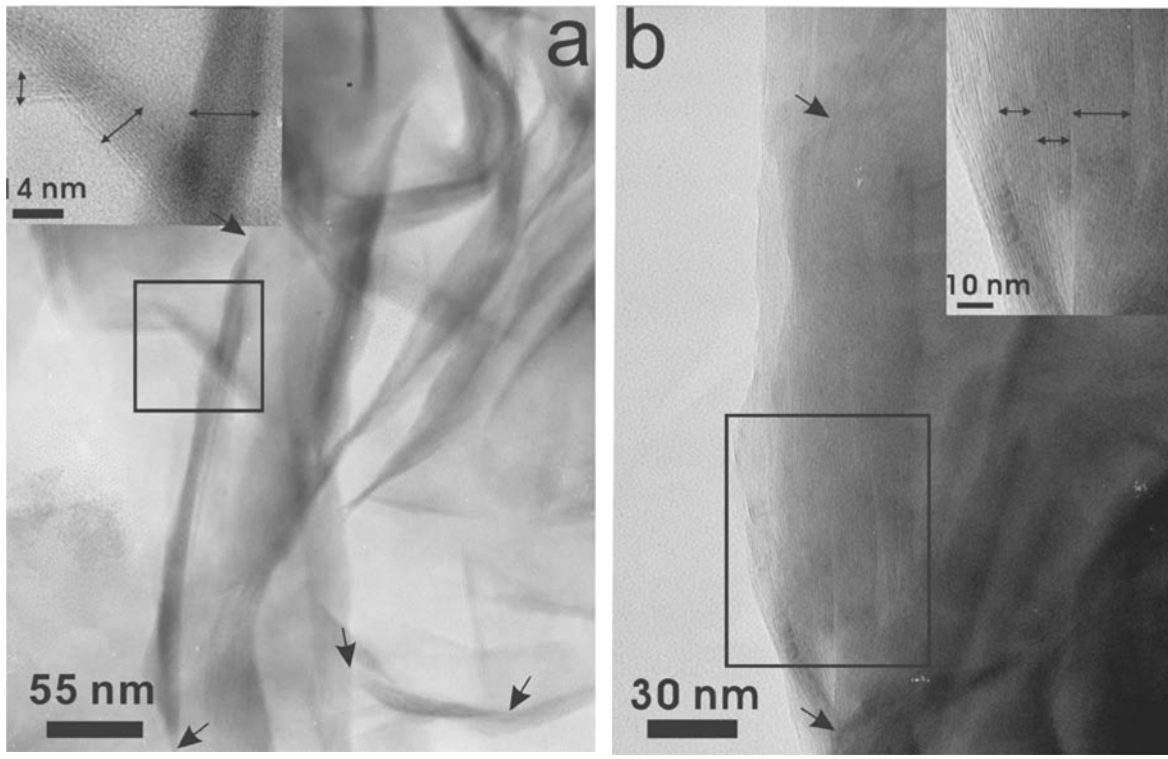


Figure 5. Direct measurement of smectite packet thickness and length on the TEM lattice-fringe images of (a) non-reduced control (NC) and (b) bioreduced smectite (BS). The boundaries of packets were defined by small angles, concentrations of edge dislocations, tapering fringes in sequences of layers, or strong image contrast. The outlined areas were enlarged to measure the packet thickness. The big arrows indicate the lengths of various smectite packets.

packets in BS (0.18 on average) compared with NC (0.11 on average) is shown in Figure 4b.

The floc architectures of NC, BS (48 h incubation), and AIS (48 h incubation) suspensions are illustrated by TEM in Figure 6. Well-dispersed smectite particles and the large open spaces are dominant features in NC (Figure 6a), whereas large clusters of randomly oriented smectite particles mixed with *S. oneidensis* (S) and less open spaces are typical in BS (Figure 6b). In the AIS suspension (Figure 6c) the particles were not aggregated as in BS and the individual smectite grains appear with open spaces similar to NC.

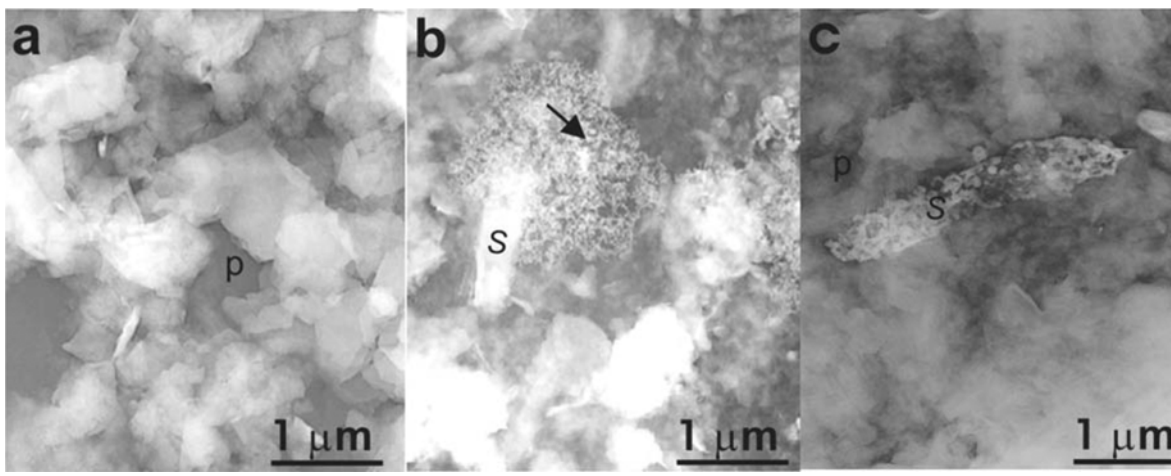


Figure 6. TEM images of (a) non-reduced control (NC) suspensions, (b) bioreduced smectite (BS) suspensions, and (c) aerobically inoculated smectite (AIS) suspensions showing the evolution in floc architecture associated with microbial Fe(III) reduction: note pore areas (p) in NC and AIS and clusters of biopolymers (see arrow) secreted by *S. oneidensis* (*S*) and smectite particles.

https://doi.org/10.1346/CCMN.2005.0530603 Published online by Cambridge University Press

Electrophoretic mobility analyses

The measured electrophoretic mobility ($m^2V^{-1}s^{-1}$) values were $(-1.8\pm0.1)\times10^{-8}$, $(-2.0\pm0.1)\times10^{-8}$, $(-1.8\pm0.2)\times10^{-8}$ and $(-2.0\pm0.1)\times10^{-8}$ for 3, 12, 24 and 48 h incubation samples, respectively. The measured electrophoretic mobility values were essentially identical for particles with different sizes (including both those which stayed in suspension after 15 min, and those which settled to the bottom of a centrifuge tube) indicating charge homogeneity for a given sample. There was no systematic change in the measured mobility with incubation time or the extent of reduction.

DISCUSSION

We have demonstrated the modification in flocculation properties of smectite suspensions, probably driven by bacterial activities, in a bench-top experiment. The clay reduction and subsequent alteration of mineral electrochemistry as well as extracellular polymeric substances (EPS) excreted by bacteria may be the predominant factors in promoting flocculation. The EPS may act as a binding agent in the flocculation process by forming polymeric bridges between the clay particles, leading to more coherent flocs. The influence of EPS on cohesive sediment stability was illustrated using low-temperature scanning electron microscopy indicating that EPS increases the tensile strength of clay minerals by the formation of polymer bridges between the clay particles (Tolhurst *et al*., 2002; Chenu and Guerif, 1991). Moreover, it has been shown that EPS fundamentally affects the physicochemical properties of cohesive sediments by increasing the molecular attractive forces between particles. For example, EPS acts as a catalyst in the flocculation process, leading to large flocs which settle more quickly (Eisma *et al*., 1983; Decho, 1990).

However, biopolymers, such as EPS, alone may not promote the flocculation of clay particles efficiently in the absence of clay reduction. In Figure 3 the aggregate-size distributions of AIS (smectite with no Fe(III) reduction + biopolymers + viable cells) and NC (smectite with no Fe(III) reduction + non-viable cells) show a similar pattern yielding finer aggregate sizes compared to that of BS (smectite with Fe(III) reduction + biopolymers + viable cells). According to the recent experiment by Beveridge (pers. comm.), EPS can be produced during growth under not only aerobic but anaerobic conditions. The production of EPS in AIS, therefore, may not play a significant role in promoting the clay flocculation as in BS. Furthermore, the increase in cell number (by a factor of ~6) was observed (not shown) by the end of 48 incubations under both aerobic and anaerobic conditions, consistent with the results from a previous study (Figure 2 in Kostka *et al*., 2002). The number of viable cells in the experiment was measured by viable cell counts. Approximately 0.1−0.2 mL of cell-clay suspension was removed from the experimental tubes, diluted and placed in an agar plate. The number of colony-forming units was counted visually. If we assume that the EPS production is proportional to cell biomass, the amount of EPS produced in AIS and BS should be similar. Therefore, it is reasonable to assume that the difference in EPS production between aerobic and anaerobic incubations is minimal and the surface charge increase induced by the microbial Fe(III) reduction may be the only variable to account for the difference in the flocculation property between AIS and BS.

The degree of clay flocculation may be controlled by surface-charge density as indicated in the ASD of BS for 3 h short-term incubation (7.2% Fe reduction) showing the intermediate pattern falling between BS for 12, 24 and 48 h long-term incubation (14.4%, 16.2% and 18% Fe-reduction, respectively) and NC (0% Fe reduction) in Figure 3. The small amount of Fe(III) reduction may cause the smaller aggregate-size distribution. An attempt at measuring the clay surface-charge density induced by the microbial Fe(III) reduction was made using micro-electrophoresis. There is no systematic change of charge density between the samples of different incubation times or different extent of reduction. The increase in the surface charge from the microbial reduction (up to 18%) may not be sufficient to be detected by the microelectrophoresis method that averages many particles and is a bulk measurement.

The direct TEM observations support the fact that the microbial activities play an important role in promoting clay flocculation. The hydrophilic Nanoplast resin (Leppard *et al*., 1996) used for TEM sample preparation does not require sample pretreatment, *e.g.* the solvent exchange process necessary in the L.R. White resin impregnation technique (Kim *et al*., 1995), which reduces the disturbance of spatial relationship between grains. Some lattice-fringe spacings of smectite were measured as 1.2 nm, but spacings varied continuously along the layers, with most layers having collapsed to 1.0 nm spacing in the TEM environment, as also observed by Ahn and Peacor (1986). As such, the measured thicknesses of smectite packets (Figure 4a) and aspect ratios would be smaller than their true values in original suspensions. Nevertheless, the increase in aspect ratio as a function of the number of layers (Figure 4b) indicates that increased face-to-face contacts of individual clay layers forms distinct thicker and longer packets as shown in Figure 5b after the microbial Fe(III) reduction, similar to the observations by Gates *et al*. (1998), causing a faster settling. Some bioreduced smectite (BS) packets also show a significant increase in the packet length after the microbial Fe(III) reduction. For example, the BS packet having a 0.2 aspect ratio and 30 layers shows a ~6-fold increase in packet length compared with a non-reduced control sample (NC) having the same aspect ratio and a much smaller number

https://doi.org/10.1346/CCMN.2005.0530603 Published online by Cambridge University Press

of layers (5). The average increase in the packet length after microbial Fe(III) reduction in this study is ~1.5 times.

The floc architecture revealed that clay particles with open spaces observed in both AIS and NC disappeared in BS due to the coalescence of clays and biopolymers. Biopolymer and clay particles are both net negatively charged and biopolymer-smectite interactions are of hydrogen bonding or exchange of the water shell of the charge-compensating cations. The aggregation of clay particles is likely to be promoted by the increased electrostatic interactions between clay particles (Gates *et al*., 1998) or by increased interactions between negatively charged clay faces and binding cations.

CONCLUSIONS

This study demonstrates that the flocculation properties of fine-grained clay suspensions are influenced and manipulated by the redox properties of clays. The benchtop experiment in this study is designed only for defining the effects of microbial Fe(III) reduction on clay flocculation in anaerobic conditions by setting all other possible variables as constant (*e.g.* salinity, temperature, disturbance, *etc*.). Oxygen-depleted environments are commonly found in the fine-grained bottom sediments of lakes, estuaries and coastal areas, as well as in the stratified water columns of nutrient-rich coastal regions and enclosed seas and lakes. Anoxic conditions are also common in sewage sludges and dredge spoils. The mobility and bioavailability of surface-active contaminants need to be considered in the context of redox-induced flocculation. We suggest that more of the variables listed above need to be considered for a future study which should seek to understand the flocculation behavior of clay particles in various natural environments.

ACKNOWLEDGMENTS

This work was supported by the Naval Research Laboratory, base program PE# 61153N (NRL contribution No. 7430-04-3). The donors of the Petroleum Research Fund, which is administered by the American Chemical Society, to HD, for partial support of this research is acknowledged. This research was also supported by a grant from National Science Foundation (EAR-0345307). We are grateful to Javiera Cervini-Silva and two anonymous reviewers for significantly improving the quality of the manuscript.

REFERENCES

Ahn, J.H. and Peacor, D.R. (1986) Transmission and analytical electron microscopy of the smectite-to-illite transition. *Clays and Clay Minerals*, **34**, 165–179.

Allison, M.A., Kineke, G.C., Gordon, E.S. and Goni, M.A. (2000) Development and reworking of a seasonal flood deposit on the inner continental shelf off the Atchafalaya River. *Continental Shelf Research*, **20**, 2267–2294.

Brassard, P. and Fish, S. (2000) The effect of divalent metals and laminar shear on the formation of large freshwater aggregates. *Hydrobiologia*, **438**, 143–155.

Chenu, C. and Guerif, J. (1991) Division s-6 sol and water management and conservation – mechanical strength of clay minerals as influenced by an adsorbed polysaccharide. *Soil Science Society of America Journal*, **55**, 1076–1080.

Decho, A.W. (1990) Microbial exopolymer secretions in ocean environments – their role(s) in food webs and marine processes. *Oceanography and Marine Biology*, **28**, 73–153.

Dong, H. (2002) Significance of electrophoretic mobility distribution to bacterial transport in granular porous media. *Journal of Microbiological Methods*, **50**, 83–93.

Dong, H., Kukkadapu, R.K., Fredrickson, J.K., Zachara, J.M, Kennedy, D.W. and Kostandarithes, H.M. (2003) Microbial reduction of structural Fe(III) in illite and goethite by a groundwater bacterium. *Environmental Science and Technology*, **37**, 1268–1276.

Droppo, I.G., Irvine, K.N. and Jaskot, C. (2002) Flocculation/aggregation of cohesive sediments in the urban continuum: Implications for stormwater management. *Environmental Technology*, **23**, 27–41.

Eisma, D., Boon, J., Groenewegen, R., Ittekkot, V., Kalf, J. and Mook, W.G. (1983) Observations on macro-aggregates, particle size and organic composition of suspended matter in the Ems Estuary. *Mitteilungen Geologisch Palaontolgische Institut der Universität Hamburg. SCOPE/UNEP Sonderband*, **55**, 295–314.

Gates, W.P., Wilkinson, H.T. and Stucki, J.W. (1993) Swelling properties of microbially reduced ferruginous smectite. *Clays and Clay Minerals*, **41**, 360–364.

Gates, W.P., Jaunet, A.M., Tessier, D., Cole, M.A., Wilkinson, H.T. and Stucki, J.W. (1998) Swelling and texture of iron-bearing smectites reduced by bacteria. *Clays and Clay Minerals*, **46**, 487–497.

Hill, P.S. (1996) Sectional and discrete representations of floc breakage in agitated suspensions. *Deep Sea Research I*, **43**, 679–702.

Hill, P.S., Voulgaris, G. and Trowbridge, J.H. (2001) Controls on floc size in a continental shelf bottom boundary layer. *Journal of Geophysical Research – Oceans*, **106**, 9543–9549.

Keeling, J.L., Raven, M.D. and Gates, W.P. (2000) Geology and characterization of two hydrothermal nontronites from weathered metamorphic rocks at the Uley graphite mine, South Australia. *Clays and Clay Minerals*, **48**, 537–548.

Keller, M.D., Bellows, W.K. and Guillard, R.L. (1988) Microwave treatment for sterilization of phytoplankton culture media. *Journal of Experimental Marine Biology and Ecology*, **117**, 279–283.

Kim, J.W. and Peacor, D.R. (2002) Crystal-size distributions of clays during episodic diagenesis: The Salton Sea geothermal system. *Clays and Clay Minerals*, **50**, 371–380.

Kim, J.W., Peacor, D.R., Tessier, D. and Elsass, F. (1995) A technique for maintaining texture and permanent expansion of smectite interlayers for TEM observations. *Clays and Clay Minerals*, **43**, 51–57.

Kim, J.W., Furukawa, Y., Daulton, T., Lavoie, D. and Newell, S. (2003) Characterization of microbially Fe(III)-reduced nontronite: environmental cell-transmission electron microscopy study. *Clays and Clay Minerals*, **51**, 382–389.

Kim, J.W., Dong, H., Seabaugh, J., Newell, S. and Eberl, D. (2004) Role of microbes in the smectite-to-illite reaction. *Science*, **303**, 830–832.

Kostka, J.E., Dalton, D., Skelton, H., Dollhopf, S. and Stucki, J.W. (2002) Growth of iron (III)-reducing bacteria on clay minerals as the sole electron acceptor and a growth yield comparison on a variety of oxidized iron forms. *Applied and Environmental Microbiology*, **68**, 6256–6262.

Kostka, J.E., Stucki, J.W., Nealson, K.H. and Wu, J. (1996)

https://doi.org/10.1346/CCMN.2005.0530603 Published online by Cambridge University Press

Reduction of structural Fe(III) in smectite by a pure culture of *Shewanella Putrefaciens* strain MR-1. *Clays and Clay Minerals*, **44**, 522–529.

Kostka, J.E., Wu, J., Nealson, K.H. and Stucki, J.W. (1999) The impact of structural Fe(III) reduction by bacteria on the surface chemistry of smectite clay minerals. *Geochimica et Cosmochimica Acta*, **63**, 3705–3731.

Kranck, K. and Milligan, T.G. (1992) Characteristics of suspended particles at an 11-hour anchor station in San Francisco Bay, California. *Journal of Geophysical Research*, **97**, 11373–11382.

Leppard, G.G., Heissenberger, A. and Herndl, G.J. (1996) Ultrastructure of marine snow. I. Transmission electron microscopy methodology. *Marine Ecology Progress Series*, **135**, 289–298.

Manning, A.J. and Dyer, K.R. (1999) A laboratory examination of floc characteristics with regard to turbulent shearing. *Marine Geology*, **160**, 147–170.

McCave, I.N. (1975) Verticla flux of particles in the ocean. *Deep Sea Research Oceanography (Abstract)*, **22**, 491–502.

Myers, C.R. and Nealson K.H. (1988) Bacterial manganese reduction and growth with manganese oxide as the sole electron acceptor. *Science*, **240**, 1319–1321.

Orton, P.M. and Kineke, G.C. (2001) Comparing calculated and observed vertical suspended-sediment distributions from a Hudson River Estuary turbidity maximum. *Estuarine Coastal and Shelf Science*, **52**, 401–410.

Stucki, J.W., Komadel, P. and Wilkinson, H.T. (1987) Microbial reduction of structural iron(III) in smectites. *Soil Science Society of America Journal*, **51**, 1663–1665.

Theilen, F.R. and Pecher, I.A. (1991) Assessment of shear strength of the sea bottom from shear wave velocity measurements on box cores and in-situ. Pp. 67–74 in: *Shear Wave in Marine Sediments* (J.M. Hoven *et al.*, editors). Kluwer Academic Publishers, The Netherlands.

Tolhurst, T.J., Gust, G. and Paterson, D.M. (2002) The influence of an extracellular polymeric substance (EPS) on cohesive sediment stability. Pp. 409–425 in: *Fine Sediment Dynamics in the Marine Environment* (J.C. Winterwerp and C. Kranenburg, editors). Elsevier, Amsterdam.

Tombacz, E., Csanaky, C. and Illes, E. (2001) Polydisperse fractal aggregate formation in clay mineral and iron oxide suspensions, pH and ionic strength dependence. *Colloid and Polymer Science*,, **279**, 484–492.

Traykovski, P., Geyer, W.R., Irish, J.D. and Lynch, J.F. (2000) The role of wave-induced density-driven fluid mud flows for cross-shelf transport on the Eel River continental shelf. *Continental Shelf Research*, **20**, 2113–2140.

Wu, J., Roth, C.B. and Low, P.F. (1988) Biological reduction of structural iron in Na-nontronite. *Soil Science Society of America Journal*, **52**, 295–296.

(*Received 15 September 2004; revised 11 July 2005; Ms. 960; A.E. Javiera Cervini-Silva*)

https://doi.org/10.1346/CCMN.2005.0530603 Published online by Cambridge University Press